Stanisław STRZELECKI*, Zdzisław SOCHA*

OPERATING TEMPERATURES OF THE BEARING SYSTEM OF GRINDER SPINDLE

TEMPERATURY PRACY UKŁADU ŁOŻYSK WRZECIENNIKA SZLIFIERKI

Key words:

theory of hydrodynamic lubrication, journal bearings, oil film temperature

Słowa kluczowe:

teoria smarowania hydrodynamicznego, łożyska ślizgowe, temperatura filmu smarowego

Abstract

The ground for the safe operation of multilobe journal bearings at proper oil film temperature is the full knowledge of bearing thermal performances particularly the oil film temperature distribution and its maximum value.

This paper describes the theoretical and experimental investigation into the operating temperatures of pericycloid, 3-lobe journal bearings

* Research Development Centre of Textile Machinery POLMATEX-CENARO, Łódź, Poland.

supporting the spindle of grinding machine. The oil film pressure, temperature and viscosity fields have been obtained by iterative solution of the Reynolds', energy and viscosity equations. Adiabatic, laminar oil film and the static equilibrium position of the journal were assumed. Experimental investigation consisted in the measurements of temperatures in the bearings.

INTRODUCTION

Hydrodynamic journal bearings can properly operate in the strictly determined range of rotational speeds. The permissible temperature of operation and the possibilities of heat conduction determine the upper boundary of the range, but the lower boundary determines the occurrence of fluid friction. The multilobe journal bearings **[L. 1–3]**, mostly used in slightly loaded, high speed rotating machines are characterised by good cooling properties, damping of vibrations and the stability. Industry applies different types of 3-lobe journal bearings. One of these types of bearings is the 3-lobe journal bearing with the pericycloid profile ("wave" bearing) **[L. 2**, **3]** that is characterised by the continuous profile of the bearing sleeve. An example of the application of such bearings is the bearing system of a grinder spindle.

The oil film temperature distribution and its maximum value are very important bearing characteristics **[L. 4–5]**. An excessive temperature of oil film causes the degradation of lubricant and bearing material. High temperature gradients may cause cracking and ratcheting, while unequal thermal growth of bearing components can cause the seizure of bearing material.

The paper describes the theoretical and experimental investigation into the operating temperatures of the journal bearings supporting the spindle of grinding machine.

The theoretical part includes the determination of oil film pressure, temperature, and viscosity distributions. These distributions were obtained from the solution of the Reynolds energy and viscosity equations. All calculations were carried-out on the assumption of adiabatic, laminar oil film and the static equilibrium position of journal. The developed code of calculations uses the finite difference method **[L. 2, 5]**.

The experimental part of the investigation consisted in the measurements of temperatures generated in the journal bearings of the grinder

spindle. The test rig was designed on the basis of a real bearing system **[L. 4]**. Each bearing of the spindle was equipped in three doubled thermocouples placed in the centre of bearing lobes about 0.2 mm below their operating surface.

GEOMETRY OF OIL FILM

The geometry of the oil film gap of pericycloid journal bearings (**Fig. 1**) is described by Equation (1) **[L. 1–3]**.

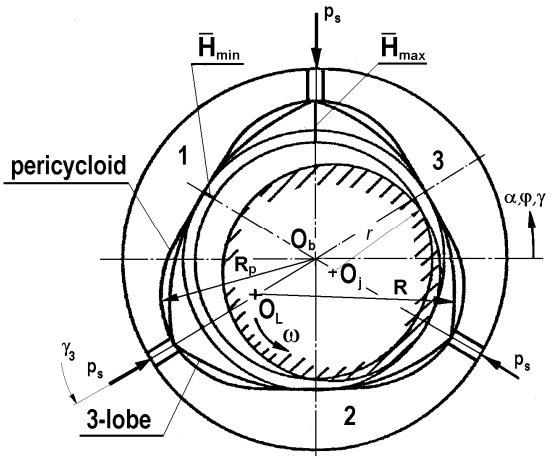

Fig. 1. Geometry of 3-lobe journal bearings; a) geometry of the oil film of 3-lobe pericycloid and 3-lobe classic journal bearings; O_b, O_j, O_L, R, r, R_p – centres and radii of bearings, journal, the lobe of classic bearing and pericycloid bearing, p_s – oil supply pressure, 1, 2, 3 – lobe number

Rys. 1. Geometria łożysk ślizgowych wielopowierzchniowych; łożysko 3-powierzchniowe z zarysem perycykloidalnym i 3-powierzchniowe symetryczne (klasyczne); O_b, O_j, O_L, R, r, R_p – środki i promienie łożysk, czopa, łożyska klasycznego i perycykloidalnego, p_s – ciśnienie zasilania olejem, 1, 2, 3 – numery segmentów

$$\overline{H} = 1 - \varepsilon \cdot \cos(\varphi - \alpha) + \lambda^* (1 + \cos n\,\varphi) \tag{1}$$

where: ε – relative eccentricity, φ – peripheral co-ordinate, α – attitude angle of centres line, λ^* pericycloid eccentricity, n – multiply of pericycloid.

OIL FILM PRESSURE AND TEMPERATURE DISTRIBUTION

The journal bearing performances for the adiabatic model of oil film can be determined by the numerical solution of the oil film geometry, and Reynolds energy and viscosity equations. The oil film pressure distribution was defined from transformed Reynolds Equation (2) **[L. 2]**.

$$\frac{\partial}{\partial\varphi}\left(\frac{\overline{H}^3}{\overline{\eta}}\frac{\partial\overline{p}}{\partial\varphi}\right)+\left(\frac{D}{L}\right)^2\frac{\partial}{\partial\overline{z}}\left(\frac{\overline{H}^3}{\overline{\eta}}\frac{\partial\overline{p}}{\partial\overline{z}}\right)=6\frac{\partial\overline{H}}{\partial\varphi}+12\frac{\partial\overline{H}}{\partial\phi} \tag{2}$$

where: D, L – bearing diameter and length (m), $\overline{H}$ = h/(R-r) – dimensionless oil film thickness, h – oil film thickness (μm), $\overline{p}$ – dimensionless oil film pressure, $\overline{p} = p\psi^2/(\eta\omega)$, p – oil film pressure (MPa), r, R – journal and sleeve radius (m), φ, $\overline{z}$ – peripheral and dimensionless axial co-ordinates, ϕ – dimensionless time, $\phi = \omega t$, t – time (sec), ω – angular velocity (sec^{-1}), $\overline{\eta}$ – dimensionless viscosity, ψ – bearing relative clearance, ψ = ΔR/R (‰), ΔR – bearing clearance, ΔR = R-r (m).

It has been assumed for the pressure region that on the bearing edges and in the regions of negative pressures the oil film pressure $\overline{p}(\varphi,\overline{z}) = 0$. The oil film pressure distribution computed from Equation (2) was put in the transformed energy Equation (3) **[L. 4, 5]**.

$$\begin{aligned}&\frac{\overline{H}}{Pe}\left[\frac{\partial^2\overline{T}}{\partial\varphi^2}+\left(\frac{D}{L}\right)^2\frac{\partial^2\overline{T}}{\partial\overline{z}^2}\right]+\left[\frac{\overline{H}^3}{12\overline{\eta}}\frac{\partial\overline{p}}{\partial\varphi}-\frac{\overline{H}}{2}\right]\frac{\partial\overline{T}}{\partial\varphi}+\left(\frac{D}{L}\right)^2\frac{\overline{H}^3}{12\overline{\eta}}\frac{\partial\overline{p}}{\partial\overline{z}}\frac{\partial\overline{T}}{\partial\overline{z}}=\\&=-\frac{\overline{H}^3}{12\overline{\eta}}\left[\left(\frac{\partial\overline{p}}{\partial\varphi}\right)^2+\left(\frac{D}{L}\right)^2\left(\frac{\partial\overline{p}}{\partial\overline{z}}\right)^2\right]-\frac{\overline{\eta}}{\overline{H}}\end{aligned} \tag{3}$$

where: $\overline{T}$ – dimensionless oil film temperature, Pe – Peclet number.

Oil film temperature and viscosity fields were obtained by numerical solving of Equation (2) and Equation (3). The temperature $T(\varphi, \overline{z})$ on the

bearing edges ($\bar{z} = \pm 1$) was computed by the method of parabolic approximation **[L. 2, 5]**. The developed program of numerical calculation **[L. 2]** solves all the above-mentioned equations.

RESULTS OF CALCULATIONS

The calculations included the non-dimensional load capacity S_0 and journal displacement ε, the static equilibrium position angles α_{eq}, and oil film pressure and temperature distributions. The assumed value of bearing length to diameter ratios was L/D = 1.0 at the bearing relative clearance $\psi = 0.4‰$ and the pericycloid relative eccentricity $\lambda^* = 0.25$. Rotational speed of journal was n = 1500 rpm. The temperature of feeding oil was equal to the ambient temperature T_0.

Calculations of oil film pressure and temperature distributions were carried out for the range of relative eccentricities ε = 0.1 to ε = 0.8. It was assumed that the load is directed vertically between the lobes (**Fig. 2** – lobe No. 2 and 3).

Exemplary results of calculated oil film pressure and temperature distributions in pericycloid 3-lobe journal bearing are showed in **Fig. 2** at the determined value of relative eccentricity ε and the static equilibrium position angle α_{eq}.

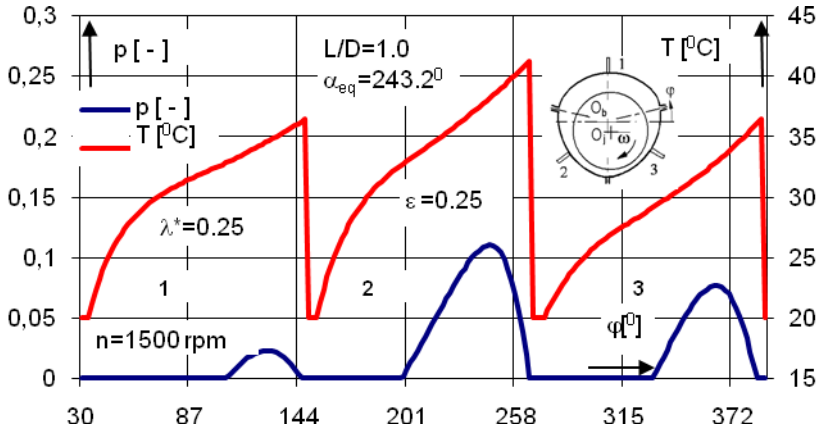

Fig. 2. Oil film pressure and temperature distribution in pericycloid 3-lobe journal bearing at determined value of static equilibrium position angle α_{eq}

Rys. 2. Rozkład ciśnienia i temperatury w filmie smarowym 3-powierzchniowego ślizgowego łożyska perycykloidalnego dla założonej wartości kąta statycznego położenia równowagi α_{eq}

In case of the load applied between the lobes of bearing, the maximum oil film pressure and temperature occur on the lobe No. 2 (**Fig. 2**). On the lobe No. 1 and No. 3, the temperatures have almost equal values (**Fig. 2**). The considered case of calculation corresponds to the load and orientation of bearing A of the grinder spindle.

EXPERIMENTAL INVESTIGATION INTO THE OIL FILM TEMPERATURE OF BEARING

The scheme of side view of the grinder spindle is showed in **Fig. 3** and the layout of spindle with the bearings, and the position of the rotor of electric motor shows **Fig. 4 [L. 4]**.

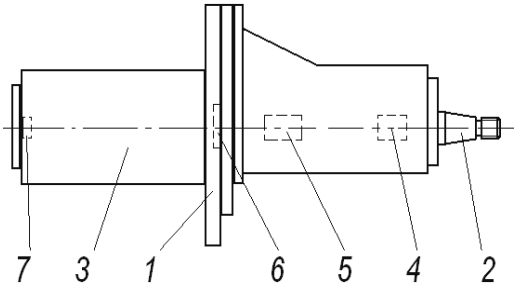

Fig. 3. Side view of test rig; 1 – casing, 2 – taper end of spindle, 3 – electric motor, 4, 5 – journal bearings, 6, 7 – rolling bearings

Rys. 3. Widok boczny stanowiska; 1 – korpus, 2 – stożek wrzeciona, 3 – silnik elektryczny, 4, 5 – łożyska ślizgowe, 6, 7 – łożyska toczne

The grinder spindle assembly (**Fig. 5** and **Fig. 6**) was fixed to the frame made of heavy grey cast elements. The schemes of the pericycloid 3-lobe journal bearings of grinding spindle are showed in **Fig. 8**. Each bearing was equipped in three doubled thermocouples NiCr-NiAl placed in the centre of bearing lobe about 0.2 mm below its surface (**Fig. 7**). Two additional thermocouples were applied for the measurements of temperatures of bearing casings. The bearings system was lubricated with the oil Velol 9 of the kinematic viscosity 9–11 mm^2/sec at 40ºC. The oil was supplied from the pressurised, central lubricating system (**Fig. 5**). The rotational speed of spindle was 1500 rpm at the rated power of electric motor 7.5 kW. The acquisition system that was coupled with the

computer has allowed for the continuous measurements of temperatures during the assumed period of time. The loading device (**Fig. 6**) has allowed for the vertical load in the upper direction by means of tightening the bolts that was fixed to the dynamometer **[L. 4]**.

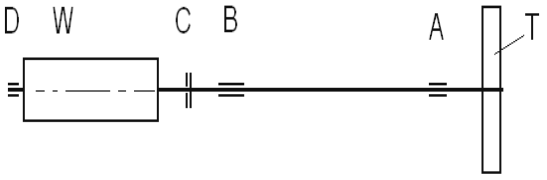

Fig. 4. Journal bearings system of the spindle of grinding machine; A, B – pericycloid 3-lobe journal bearings, C – axial ball bearing, D – deep groove ball bearing, W – rotor of electric motor, T – grinding wheel

Rys. 4. Układ łożysk ślizgowych wrzeciennika; b A, B – 3-powierzchniowe łożyska z zarysem perycyckloidalnym, C – łożysko wzdłużne, D – łożysko kulkowe, W – wirnik, T – ściernica

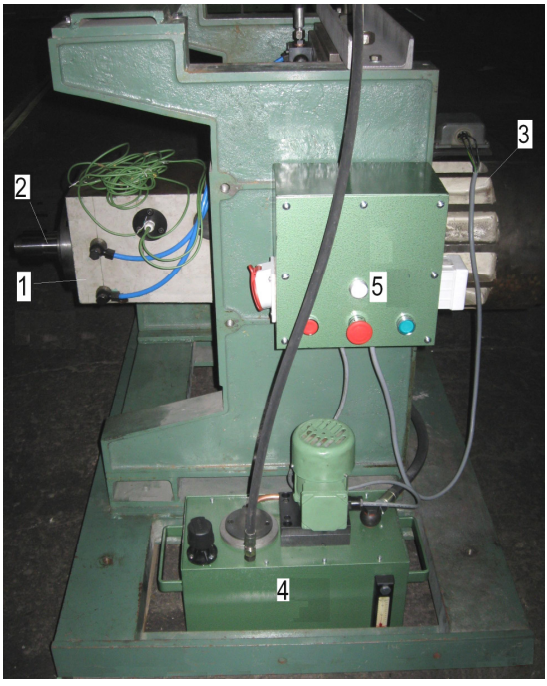

Fig. 5. Side view of the spindle assembly of grinding machine SPE-40; 1 – casing, 2 – spindle, 3 – electric motor, 4 – oil supply system, 5 – control system

Rys. 5. Widok boczny stanowiska badawczego temperatury pracy łożysk wrzeciennika szlifierki SPE-40; 1 – korpus, 2 – wrzeciono, 3 – silnik elektryczny, 4 – układ zasilania olejem, 5 – układ sterowania

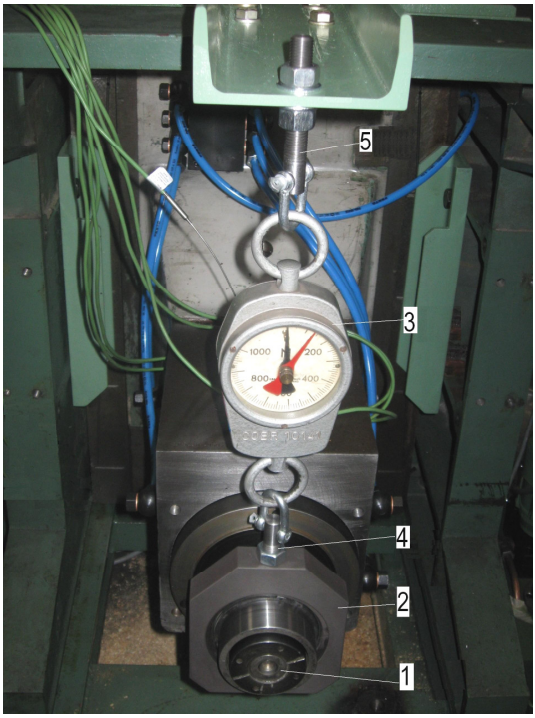

Fig. 6. Face view of the spindle assembly with the loading device; 1 – spindle, 2 – casing of ball bearing, 3 – dynamometer, 4 – grip, 5 – upper grip

Rys. 6. Widok czołowy stanowiska z układem obciążania łożysk wrzeciennika; 1– wrzeciono, 2– obudowa łożyska tocznego, 3 – dynamometr, 4 – uchwyt, 5 – uchwyt górny

The temperature measuring system consists of the following elements (**Fig. 8**):

1. Grinding spindle assembly — JOTES
2. Card SENSOR — SENSOR,
3. Notebook AMILO L1300 — Fujitsu-Siemens,
4. Thermocouples TP-203K — CZAKI
5. Amplifiers modules of thermocouples of K type — SENSOR,
6. Measuring card DAQcard-6024E — National Instruments,
7. Program of measuring card NIDAQ740 — National Instruments,
8. Program of data acquisition KSD-400 — SENSOR.

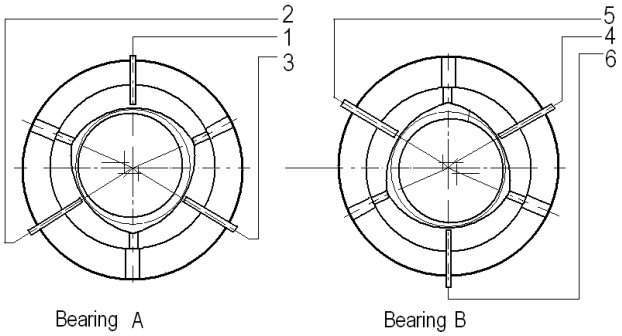

Fig. 7. Arrangement of thermocouples in the pericycloid 3-lobe journal bearings of the spindle of grinding machine SPE-40

Rys. 7. Układ czujników temperatury w łożyskach 3-powierzchniowych z zarysem perycykloidalnym wrzeciennika szlifierki SPE-40

The series of the measurements consisting of 192 readings were made every 2 seconds. In each series, the temperature measurement was made in 6 points 32 times. The results that are showed in **Fig. 9** include 3400 series of measurements.

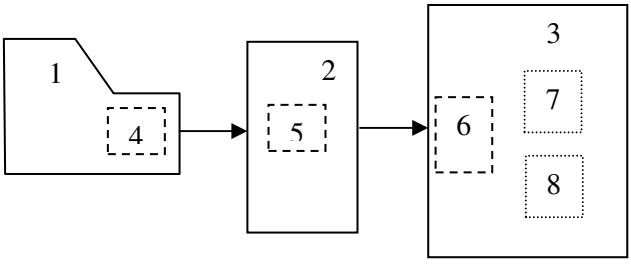

Fig. 8. Layout of the temperature measuring system applied for the grinding spindle journal bearings

Rys. 8. Układ pomiarowy temperatury łożysk wrzeciennika

Exemplary results of operating temperature measurements are showed in **Fig. 9**. It results from **Fig. 9** that the lowest temperature was registered on the lobe No.3 of A bearing and the highest on the lobe No. 5 of B bearing (**Fig. 7**).

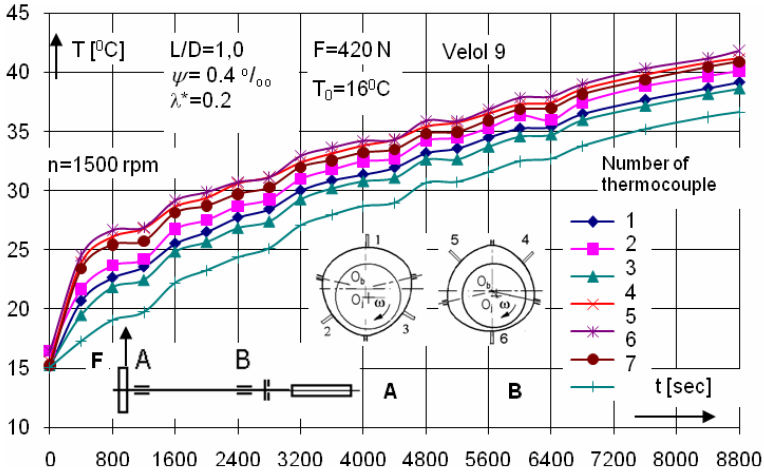

Fig. 9. Runs of temperatures measured on the operating surfaces of the pericycloid 3-lobe journal bearings of grinding spindle SPE-40; thermocouple No. 7 – casing of bearing A

Rys. 9. Przebiegi temperatur mierzonych na powierzchniach roboczych łożysk 3-powierzchniowych z zarysem perycykloidalnym wrzeciennika SPE-40; czujnik temperatury nr 7 – obudowa łożyska A

FINAL REMARKS

The paper summarises the results of the calculations and experimental investigation of the oil film temperatures of pericycloid 3-lobe journal bearings that were applied in the real mechanical system of the grinding spindle. The calculated temperatures were obtained for a single bearing. In a real bearing system, the temperatures of oil film are affected by many factors, e.g., casing design, temperature of supplied oil and its pressure. However, the results that were obtained from the theory and experiment show the correct values on the bearing lobes. There is good agreement in, e.g. maximum oil film temperatures on the operating lobes of bearings (**Fig. 2** and **Fig. 9**). In the steady-state conditions of grinder spindle operation, the measured temperatures are in the range of 38–42ºC (**Fig. 9**), and they correspond to the calculated temperatures (**Fig. 2**).

Experimental investigations certify the correct operation of developed code of calculations.

Rewiever
Jan SIKORA

Streszczenie

Wielopowierzchniowe łożyska ślizgowe [L. 1–3], stosowane są w lekko obciążonych, wysokoobrotowych maszynach wirnikowych. W praktyce stosowane są łożyska ślizgowe 3-powierzchniowe z perycykloidalnym zarysem panewki (łożysko „falowe" – „wave") [L. 2, 3]. Przykładem ich zastosowania jest układ łożyskowania wrzeciennika szlifierki lub łożyska satelitów przekładni planetarnej [L. 3].

W części teoretycznej wyznaczono rozkłady ciśnienia i temperatury w filmie smarowym 3-powierzchnowego łożyska z zarysem perycykloidalnym rozwiązując równania Reynoldsa, energii i lepkości środka smarowego. Obliczenia przeprowadzono metodą różnic skończonych [L. 2] dla przypadku adiabatycznego filmu.

W doświadczalnej części badań pomierzono temperatury na powierzchniach roboczych 3-powierzchniowych łożysk z zarysem perycykloidalnym. Stanowisko badawcze skonstruowano na bazie rzeczywistego układu łożysk ślizgowych [L. 4]. Każde z łożysk ślizgowych wyposażono w trzy czujniki temperatury umieszczone w środkowej płaszczyźnie łożyska w odległości około 0,2 mm od powierzchni roboczej panewki. Pomierzone wartości temperatur porównano z wartościami wyznaczonym teoretycznie.